Research Article

Wenjie Sun* and Xiaobin Tang

Nonlinear structural and vibration analysis of straddle monorail pantograph under random excitations

https://doi.org/10.1515/nleng-2025-0104
received January 14, 2025; accepted March 3, 2025

Abstract: The dynamic behavior of the straddle monorail pantograph system is significantly influenced by nonlinearities arising from its unique structural configuration and operational environment. This article presents a mathematical model that incorporates both nonlinear geometric and material properties of the pantograph. A finite element model is utilized to perform modal and static analyses, identifying stress concentrations and dynamic characteristics. To account for random vibration excitations, a nonlinear dynamic response framework is developed, considering vehicle-induced vibrations and network irregularities as stochastic excitation sources. The results demonstrate that these nonlinearities amplify specific resonances under random excitation, leading to increased stress and deformation at critical points. These findings provide a foundation for enhancing fault detection strategies and designing more robust pantographs, with nonlinear vibration monitoring proposed as an effective diagnostic tool. This study contributes to both theoretical understanding and practical improvements in ensuring the reliability and longevity of straddle monorail systems.

Keywords: nonlinear dynamics, random vibration, straddle monorail pantograph

*** Corresponding author: Wenjie Sun**, College of Traffic and Transportation, Chongqing Jiaotong University, Chongqing, 400074, China; Chongqing Vocational Institute of Engineering, Chongqing, 402260, China, e-mail: syycq2024@163.com
Xiaobin Tang: Chongqing Vocational Institute of Engineering, Chongqing, 402260, China

1 Introduction

The pantograph of a straddle monorail vehicle is a critical component responsible for stable energy transmission, ensuring the proper functioning of various systems. Unlike traditional railway or subway pantographs, the straddle monorail pantograph is mounted laterally on the bogie, resulting in unique structural and dynamic behaviors [1–3]. This distinct configuration introduces nonlinearities into the system's dynamic response, including nonlinear stiffness, damping effects, and geometric constraints. Despite its importance, the operational lifespan of the pantograph in many real-world settings is often much shorter than its designed lifespan, leading to costly failures, service interruptions, and safety risks [4–7].

In recent years, research on straddle monorail pantographs has gradually increased, focusing primarily on nonlinear dynamics and random vibration analysis. However, most existing studies focus on high-speed rail and subway pantograph systems, with limited attention given to the unique nonlinear dynamic characteristics of straddle monorail pantographs. In particular, the coupling effects of geometric and elastic nonlinearities, as well as the impact of random vibrations on pantograph lifespan, have not been thoroughly explored. Therefore, this study aims to fill this research gap by developing a nonlinear mathematical model and conducting finite element analysis to investigate the dynamic behavior of straddle monorail pantographs under random excitations [8–10].

To address these challenges, this article investigates the nonlinear dynamic behavior of the straddle monorail pantograph under random vibration excitations. A mathematical model that integrates nonlinear geometric and material properties is developed, providing insights into the coupled vibrational modes. Finite element model (FEM) is employed to identify stress concentration points and examine how nonlinearities influence vibration modes and structural integrity under operational conditions. Random vibration analysis is performed using stochastic differential equations

to model the pantograph's response to excitation sources, such as vehicle body vibrations and contact network irregularities. The nonlinearities in the system significantly affect its resonance characteristics, leading to localized stress amplification. These effects are crucial for understanding failure mechanisms and developing robust monitoring and fault detection strategies.

This study aims to fill the gap in understanding the nonlinear dynamics of straddle monorail pantographs. By integrating nonlinear modeling, finite element analysis, and random vibration theory, the research provides a comprehensive framework for analyzing and improving the reliability of pantograph systems in urban transit. The findings are expected to inform the design of next-generation pantographs and establish advanced fault detection methodologies, leveraging nonlinear vibration signals as diagnostic tools.

2 Nonlinear mathematical model of a straddle monorail pantograph methodology

The straddle monorail pantograph consists of several key components, including the bottom plate, upper and lower frames, connecting rod, balance rod, and bow head assembly. Due to its installation location on the vehicle, its vibration primarily occurs in the lateral direction [11–15]. Based on this configuration, the pantograph is simplified into a two-dimensional rigid body dynamic system consisting of interconnected members, as shown in Figure 1.

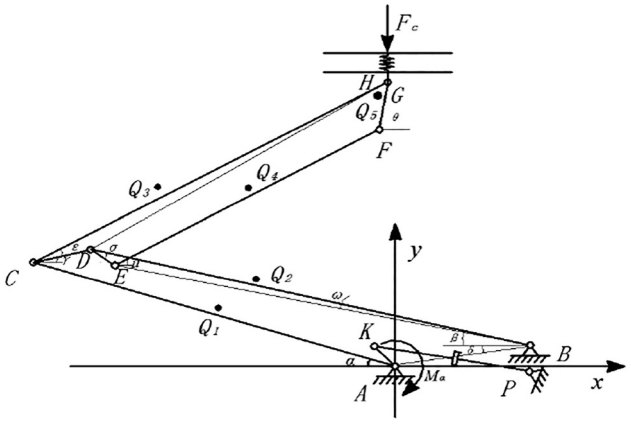

Figure 1: Simplified two-dimensional model of the straddle monorail pantograph.

Main components:

(1) Lower frame: Simplified as rod *AC*.
(2) Connecting rod: Represented by rod *BDE*.
(3) Upper frame: Simplified as rod *CDG*.
(4) Balance rod: Modeled as rod *EF*.
(5) Bow head support: Represented as rod *FGH*.

Hinge points:

(1) *A, C:* hinge points between the lower frame, bottom plate, and upper frame.
(2) *B, D, E:* hinge points connecting the bottom plate, upper frame, and balance rod.
(3) *E, F, G, H:* hinge points for the balance rod, upper frame, and bow head support.

Elastic element:

(4) *K, P:* The two ends of the pantograph spring, connected to the lower frame and bottom plate, respectively.
(5) $\alpha, \beta, \gamma, \theta$: Angles between rods *AC, BD, CD, AB* and the *x*-axis.
(6) δ, ϕ: Angles between rods *CD* and *DG*, as well as FG and the *x*-axis.

The system is modeled in a two-dimensional plane, with motion constrained to the *x*–*y* plane. The gravity direction is assumed to align with the negative *z*-axis.

To simplify the derivation:

(1) Point *A* is chosen as the origin of the coordinate system.
(2) The vehicle's running direction is along the positive *x*-axis, while the lateral vibration direction is along the positive *y*-axis.
(3) The longitudinal displacement and rotational angles of the bow head are negligible, with the motion predominantly occurring in the *y*-direction.

The model incorporates nonlinearities arising from:

(1) Geometric nonlinearities: due to the changing angles between rigid members during motion.
(2) Elastic nonlinearities: from the spring and damping elements connected to the bow head.
(3) Contact nonlinearities: at the interface between the bow head and the contact network.

The positions of the hinge points are determined by geometric constraints. For example:

$$x_D = x_C + L_{CD}\cos\gamma,\quad y_D = y_C + L_{CD}\sin\gamma,$$

$$x_E = x_D + L_{DE}\cos\delta,\quad y_E = y_D + L_{DE}\sin\delta,$$

$$x_H = x_F + L_{FH}\cos\phi,\quad y_H = y_F + L_{FH}\sin\phi.$$

The displacements of all hinge points are expressed in terms of the generalized coordinates y_H, x_F, y_F, and θ_F.

Nonlinear differential equation for the bow head: the bow head is subject to the following forces:

(1) Elastic force: $F_{KH} = k_H(y_H)y_H$, where $k_H(y_H)$is the nonlinear stiffness of the elastic element.
(2) Damping force: $F_{dH} = c_H(y_H, \dot{y}_H)\dot{y}_H$, where c_H is the nonlinear damping coefficient.
(3) Contact force: F_c, which depends on the contact condition with the network.

Applying Newton's second law in the y-direction:

$$m_H\ddot{y}_H = F_c - F_{dH} - F_{kH}.$$

Substituting the expressions for F_{kH} and F_{dH}:

$$m_H\ddot{y}_H + c_H(y_H, \dot{y}_H)\dot{y}_H + k_H(y_H)y_H = F_c.$$

This nonlinear equation describes the vertical motion of the bow head.

Nonlinear equations for the frame: the frame's dynamics include translational motion in the x and y directions and rotational motion about its center of mass:

Translational motion:

$$m_F\ddot{x}_F + c_F(x_F, \dot{x}_F)\dot{x}_F + k_F(x_F)x_F = F_{\text{frame},x},$$

$$m_F\ddot{y}_F + c_F(y_F, \dot{y}_F)\dot{y}_F + k_F(y_F)y_F = F_{\text{frame},y}.$$

Rotational motion:

$$I_F\ddot{\theta}_F + c_\theta(\theta_F, \dot{\theta}_F)\dot{\theta}_F + k_\theta(\theta_F)\theta_F = M_{\text{frame}},$$

where I_F is the rotational inertia, c_θ and k_θ are the rotational damping and stiffness coefficients, and M_{frame} is the net moment acting on the frame.

Comprehensive nonlinear dynamic model

Combining the equations for the bow head and the frame, the system's generalized equation of motion is as follows:

$$M(q)\ddot{q} + C(q, \dot{q})\dot{q} + K(q)q + F_{\text{nonlinear}} = F_{\text{external}},$$

where $q = [x_F, y_F, \theta_F, y_H]$: generalized coordinate vector; *M, C, K:* Mass, damping, and stiffness matrices incorporating nonlinear terms; $F_{\text{nonlinear}}$: nonlinear force vector accounting for geometric, elastic, and contact nonlinearities; and F_{external}: external excitation from the vehicle and contact network.

The nonlinear mathematical model reveals a close correlation between the vibration characteristics and structural condition of the pantograph. Key parameters, including natural frequencies, vibration amplitudes, modal shapes, and local stress/strain distribution, serve as critical indicators of structural damage. Natural frequencies are determined by the stiffness and mass of the system, and structural damage (*e.g.*, stiffness degradation or loosened connections) results in a reduction of natural frequencies. Vibration amplitudes are influenced by nonlinear stiffness and damping properties, with structural damage amplifying vibrations at critical locations. Modal shapes exhibit significant changes in deformation at damaged regions, and abnormal increases in local stress or strain distribution directly indicate structural damage. By monitoring vibration data and analyzing the changes in these parameters, structural damage in the pantograph can be effectively identified and localized, providing theoretical support for optimizing structural design and improving operational reliability.

Figure 2: Fracture in the lower frame.

Through actual investigation, the structural damage of monorail vehicle pantograph is mainly concentrated on the upper and lower frames, as shown in Figures 2 and 3.

3 Finite element analysis of straddle monorail pantograph

A key condition to ensure reliable current collection for monorail vehicles is the consistent and effective contact between the pantograph and the contact line. During

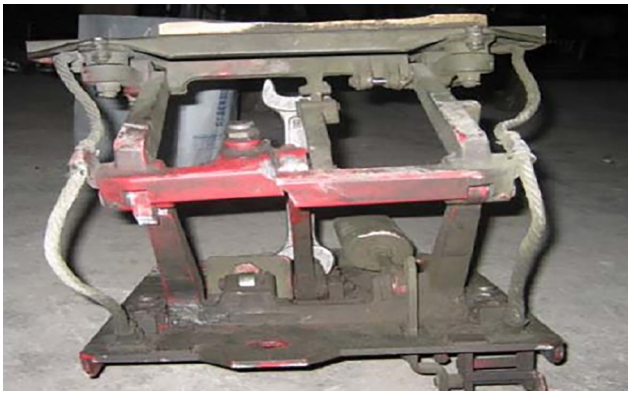

Figure 3: Fracture in the upper frame.

operation, the pantograph undergoes a total extension (in the upward direction) and compression (in the downward direction) ranging from 160 mm to 300 mm, with a standard operating height of 230 mm. At this height, the contact pressure of the pantograph is 59 N. To maintain effective current collection, the contact pressure must satisfy the following conditions:

(1) In the elongation direction: the contact pressure should exceed 44 N.
(2) In the compression direction: the contact pressure should remain below 78 N.

Excessive contact pressure increases abnormal wear on both the pantograph and the contact wire, significantly reducing their service life. Conversely, insufficient contact pressure leads to poor interaction between the pantograph and the contact line, resulting in intermittent power supply. This can further cause sparks or arcs, leading to localized burning of the contact wire.

Model simplifications and boundary conditions

The pantograph is composed of multiple interconnected rods, each connected at specific hinge points. However, during the stress analysis of different working positions, the degrees of rotational freedom between these rods are ignored, assuming rigid connections at a specific position. As a result, the pantograph can be simplified for analysis as a system of individual components with fixed geometric constraints.

To accurately simulate the stress distribution in the pantograph:

(1) Boundary conditions: a fixed constraint is applied to the bottom surface of the base plate, representing its attachment to the monorail vehicle.
(2) Load conditions: the contact force and operational constraints are applied as shown in Figure 4. This includes the upward and downward forces resulting from the pantograph's interaction with the contact wire and the elastic forces within the system.

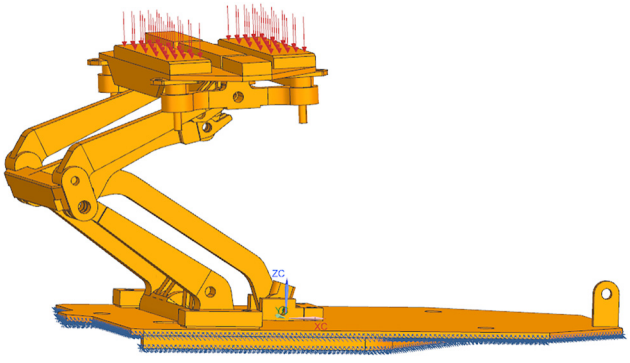

Figure 4: Load and constraint condition of pantograph.

The simplified model and boundary conditions for the finite element analysis are illustrated in Figure 4, where the fixed constraint and load distribution represent the real-world operational conditions.

3.1 Modal analysis of straddle-type monorail pantograph

Modal analysis is an essential tool for investigating the dynamic characteristics of a system, and it can be classified into theoretical modal analysis and experimental modal analysis based on the research approach. Theoretical modal analysis, also referred to as the analytical process, establishes the relationship between external excitations, the system's dynamic behavior, and its response, based on linear vibration theory. It integrates vibration theory, dynamic testing, digital signal processing, and parameter identification for systematic recognition of the system's modal parameters. Experimental modal analysis, on the other hand, involves physical testing to determine modal parameters. While valuable for verifying and comparing theoretical models, it is time-consuming, labor-intensive, and costly, making it unsuitable for early-stage product design and development. Thus, experimental modal analysis is typically used for post-design validation.

This study employs a theoretical modal analysis approach to evaluate the dynamic characteristics of the straddle-type monorail pantograph. The analysis leverages vibration theory and focuses on extracting critical modal parameters. A FEM of the pantograph is used as the foundation, with loads applied according to the international electrotechnical commission (IEC) 61373-2010 standard. The modal analysis is conducted under the standard operating height of H = 230 mm, representing the normal working position of the pantograph. The structural parameters of each pantograph component are listed in Table 1, which ensures that the model comprehensively reflects the real-world dynamic behavior of the system.

Table 1: Parameters of pantograph

Part	Material	Mass (kg)
Bowhead	Aluminum alloy	0.519
Copper slider	Copper alloy	0.831
Archehead seat	Aluminum alloy	1.68
Upper frame	Aluminum alloy	0.732
Stabilizer bar	Aluminum alloy	0.087
Lower frame	Aluminum alloy	0.151
Stabilizer bar	Aluminum alloy	0.237

In this analysis, the first six modes corresponding to rigid body motion are excluded due to their negligible contribution to structural deformation. Instead, the analysis focuses on the 7th to 12th modes, which provide critical insights into the system's structural dynamics. The results of the modal analysis, including natural frequencies and mode shapes, are presented in Table 2 and illustrated in Figure 5. These results highlight key structural vibration modes, including the deformation characteristics of the upper and lower frames, connecting rods, and bow head. This information is crucial for identifying potential resonance risks and stress concentration areas in the pantograph.

The modal analysis reveals that the dynamic performance of the pantograph is heavily influenced by the natural frequencies of its key modes. Areas of significant deformation correspond to regions of high dynamic stress, particularly in the upper and lower frame connections and hinge points. Such insights provide valuable guidance for optimizing the pantograph's structural design, particularly in mitigating resonance and enhancing fatigue resistance. The findings further emphasize the importance of balancing stiffness and mass distribution across the pantograph to avoid critical frequencies that may lead to excessive vibration or structural failure under operational conditions.

The structural vibration modes reveal the inherent vibration characteristics of the pantograph. Analyzing the 7th- to 12th-order modes, the maximum equivalent stress values and their corresponding locations were identified as follows:

7th mode: maximum equivalent stress is 213.99 MPa, located at the connection between the lower frame and the upper frame.

8th mode: maximum equivalent stress is 277.04 MPa, occurring at the connection between the upper frame and the pantograph head.

9th mode: maximum equivalent stress is 267.24 MPa, concentrated at the connection between the lower frame and the upper frame.

10th mode: maximum equivalent stress is 234.69 MPa, again occurring at the connection between the lower frame and the upper frame.

Table 2: FEM analysis results of pantograph

Modal order	Displacement Max (mm)	Stress Max (MPa)
Mode 7	1.213	213.99
Mode 8	1.425	277.04
Mode 9	2.300	267.24
Mode 10	1.260	234.69
Mode 11	1.728	281.60
Mode 12	1.910	406.09

11th mode: maximum equivalent stress is 281.60 MPa, located at the connection between the lower frame and the upper frame.

12th mode: maximum equivalent stress is 406.09 MPa, concentrated at the connection between the bottom plate and the lower frame.

In summary, the connections between the lower frame, the upper frame, and the bottom plate are the weaker points in the pantograph structure. Across the 7th–12th modes, the maximum equivalent stress ranges from 213.99 to 406.09 MPa. In some cases, the stress values approach or exceed the material's strength limit, increasing the risk of structural failure.

3.2 Static analysis of straddle-type monorail pantograph

The structure and contact force of the straddle-type monorail pantograph vary across different working positions. A static analysis was performed to evaluate the force conditions of the pantograph at three critical positions: the highest working position (H = 300 mm), the normal working position (H = 230 mm), and the lowest working position (H = 160 mm). The structural characteristics of the pantograph at these working heights are summarized in Table 3, and the results of the static analysis are presented in Figure 6.

Based on the aforementioned analysis, the maximum equivalent stress of the pantograph is primarily concentrated at the connection between the lower frame and the upper frame, as well as at the eccentric region near the bearing frame of the upper frame. This region is critical as it connects the upper frame, the stabilizer bar, and associated components, resulting in a structurally complex and highly stressed area. Consequently, it is more prone to damage compared to other locations.

4 Random vibration analysis of straddle-type monorail pantograph

The straddle-type monorail pantograph is an elastic vibration system installed at the lower part of both sides of the vehicle body. During vehicle operation, it is subjected to various excitation forces and disturbances. These excitation sources can be categorized into two main types: vibrations originating from the vehicle body and those arising from the contact network.

The first category, vibration sources from the vehicle body, includes:

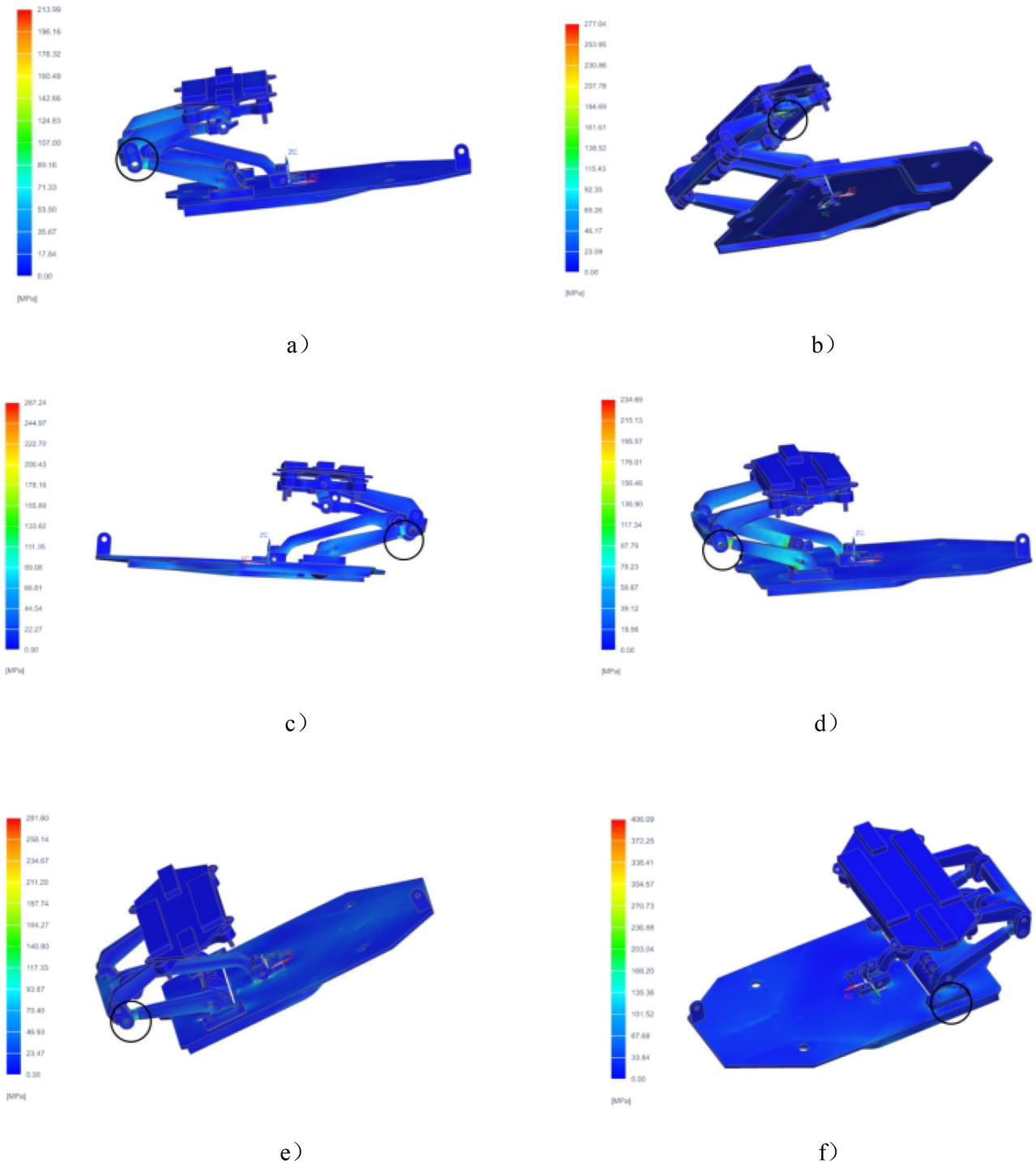

Figure 5: Distribution of maximum values of 7th–12th-order vibration-equivalent stress of pantograph: (a) 7th-order vibration mode, (b) 8th-order vibration mode, (c) 9th-order vibration mode, (d) 10th-order vibration mode, (e) 11th-order vibration mode, and (f) 12th-order vibration mode.

(1) Vibration from the vehicle power system;
(2) Vibrations caused by the track structure;
(3) Irregularities between wheels and tracks, with wheel-rail irregularity being the primary cause of wheel-rail vibrations.

The second category of vibrations originates from the contact network. Over prolonged operation, accumulated deformation in the contact network results in uneven contact surfaces, which induce harmful vibrations between the pantograph and the rigid catenary. These vibrations

Table 3: Structural characteristics of pantograph at different working heights

Height	H300 mm	H230 mm	H160 mm
Angle between the upper frame and the bow head	43.600	29.600	14.000
Angle between the lower frame and the bottom plate	49.300	39.960	24.130
Angle between the connecting rod and the base plate	38.240	28.340	17.060

not only degrade the current collection quality but also pose serious risks to the safe operation of urban rail transit, potentially leading to pantograph fractures. The irregularity of the contact surface is inherently a stochastic process. When viewed as part of an infinite rigid catenary system, it can be treated as a stationary stochastic process, representing a source of random excitation for the pantograph–catenary system.

If the frequency of these excitations coincides with one of the pantograph's natural frequencies, resonance will occur, generating large resonant dynamic loads at certain locations within the pantograph structure. This phenomenon results in high equivalent stress, shear stress, and deformation, increasing the risk of structural damage to the pantograph. The uncertain, time-varying nature of these loads is referred to as random loads. The motion of a multi-degree-of-freedom system under stationary random external forces can be described by the following equation:

$$M\ddot{u}_F(t) + C\dot{u}_F(t) + Ku(t) = F(t),$$

where M is the mass matrix of the system, C is the damping matrix, K is the stiffness matrix, $\ddot{u}(t)$ is the system's acceleration, $\dot{u}(t)$ is the system's velocity, and $F(t)$ is the random external load acting on the system due to displacement $u(t)$.

Unlike deterministic vibrations, random vibrations follow probabilistic statistical laws and must be analyzed using statistical methods. The stochastic nature of the system necessitates

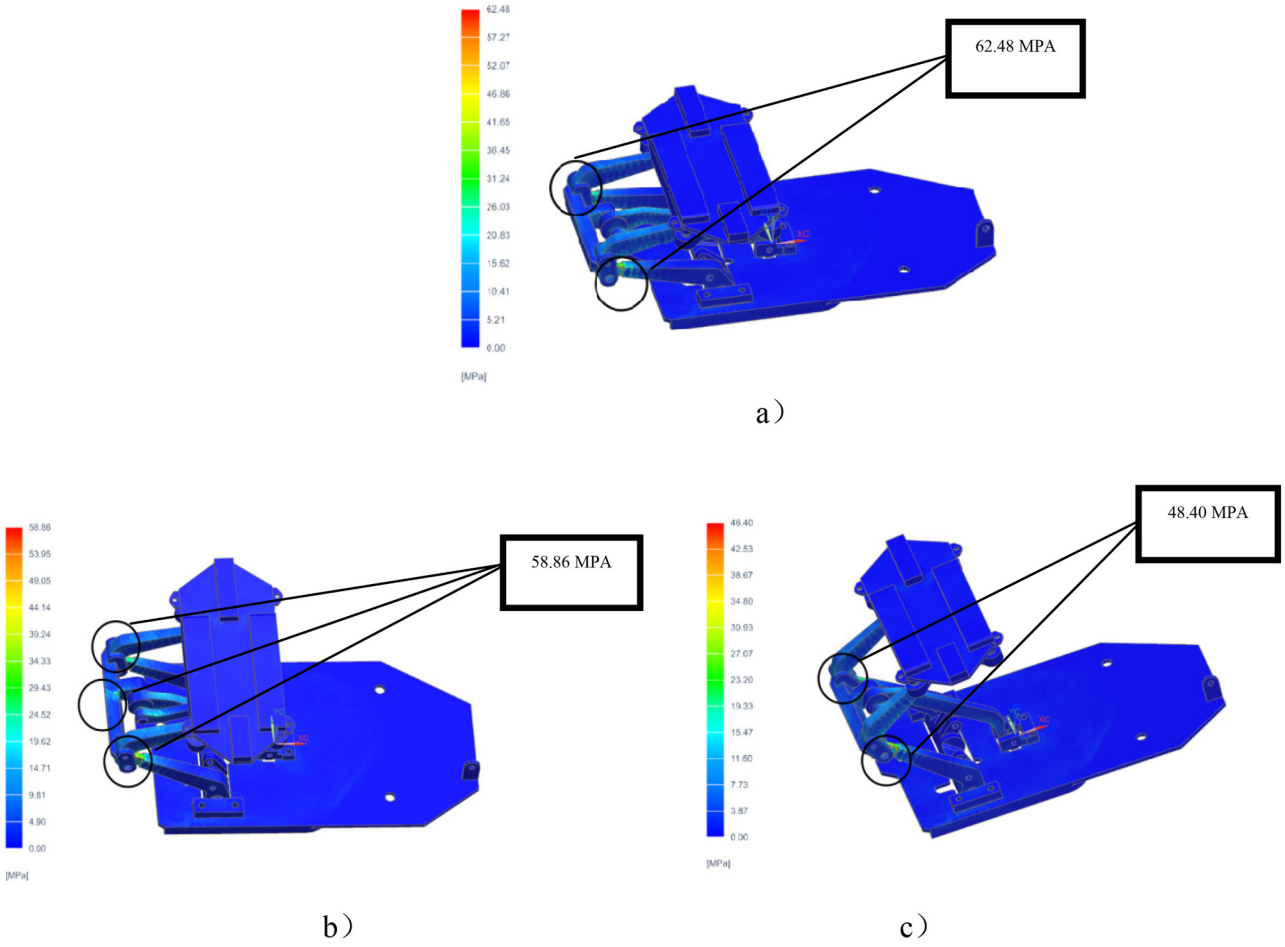

Figure 6: Equivalent stress diagram of pantograph at three positions: (a) H160 mm working position, (b) H230 mm working position, and (c) H300 mm working position.

Table 4: Summary of root mean square acceleration levels

Category	Maximum horizontal root mean square (m/s2)	Mean square root of average level (m/s2)
Vertical	7.0	3.1
Transverse	7.0	3.0
Direction	4.1	1.2

consideration of statistical distributions for responses such as stress and deformation.

The IEC 61373-2010 standard provides guidance for vibration analysis by classifying equipment based on its installation location (vehicle body, bogie, or axle). Since the straddle-type monorail pantograph is installed on the bogie, the corresponding load conditions must be applied for vibration analysis. According to the standard, the random load values for the pantograph are provided in Table 4.

To evaluate the behavior of the pantograph under random vibration, the following conditions were simulated:

(1) Normal condition: the pantograph is in the H230 mm standard operating position, with all components intact.
(2) Simulated fault condition: the pantograph is in the H230 mm standard operating position, but with a modeled fracture at locations identified as prone to failure in the prior structural analysis.

Simulation results under these two conditions are presented in Figure 7. The analysis demonstrates that under normal conditions, the stress and deformation are well

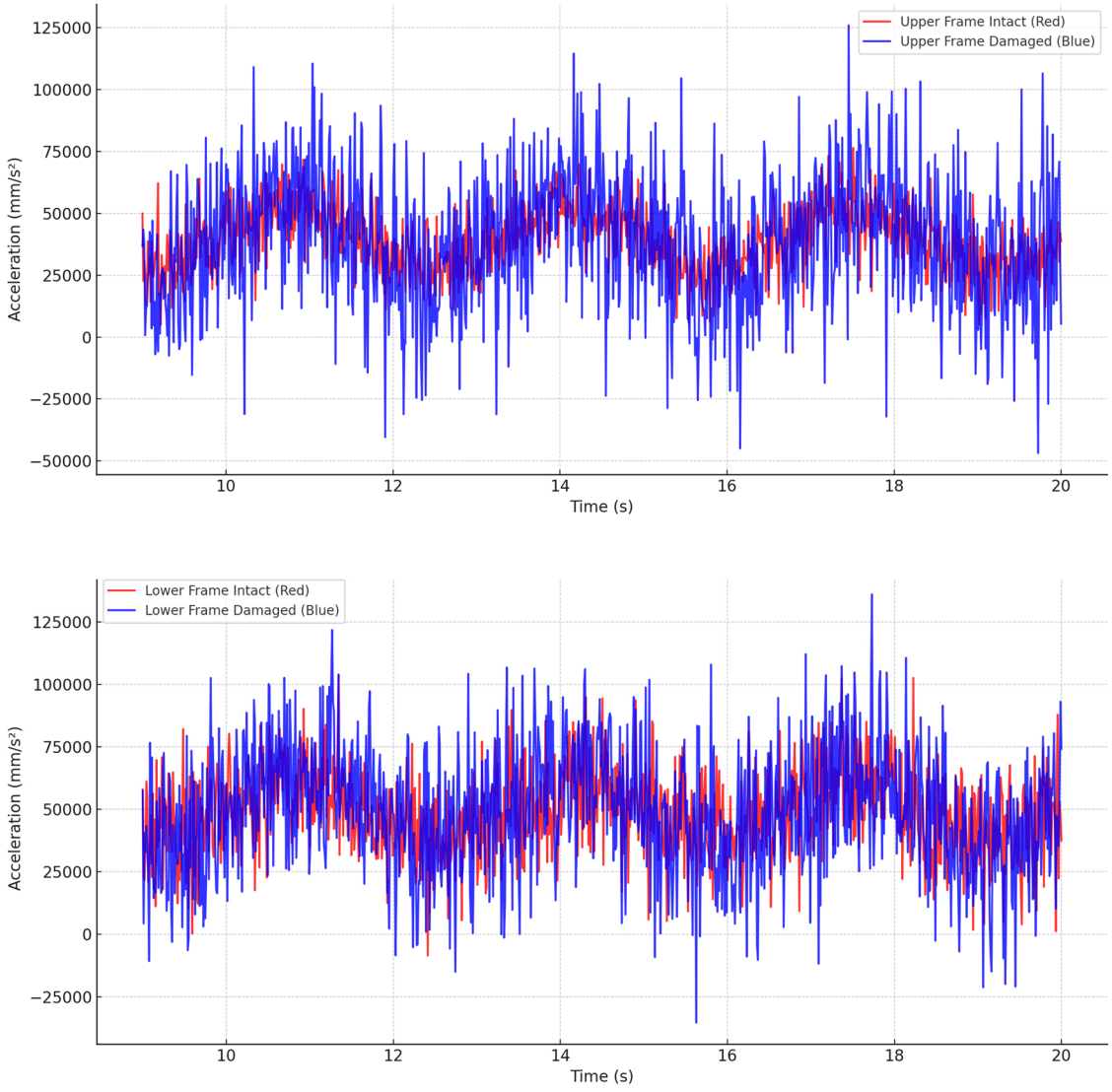

Figure 7: Acceleration chart of pantograph: (a) acceleration chart of cracks generated in weak links of upper frame of pantograph under normal state and simulation and (b) acceleration chart of cracks in weak links of lower frame of pantograph under normal state and simulation.

distributed and remain within safe operational limits. However, in the simulated fault condition, significant stress concentrations and large deformations were observed near the fracture-prone regions. These results confirm that random vibrations, particularly under fault conditions, exacerbate the risk of failure in structurally weak areas, such as the connections between the lower frame, upper frame, and bottom plate.

In the normal state, the red line represents the acceleration signals of the upper and lower frames in an intact condition, with smaller and more uniform fluctuations, reflecting the structural stability. In the damaged state, however, the blue line shows significantly increased and more irregular fluctuations in the acceleration signals of the upper and lower frames, indicating dynamic instability caused by structural damage. A clear comparison reveals that the acceleration signals exhibit significant changes in the damaged state, including higher amplitudes and more chaotic fluctuation patterns. This result validates the reliability and effectiveness of using vibration signal analysis to detect structural damage in the pantograph.

5 Conclusion and outlook

This study develops a comprehensive mathematical model for the straddle-type monorail pantograph, offering a detailed analysis of its dynamic and structural behaviors. The findings demonstrate that the horizontal and longitudinal vibrations of the pantograph are closely linked to its structural parameters, highlighting the significance of understanding the interaction between dynamic forces and structural characteristics. Using the FEM, a detailed FEM of the pantograph was established to conduct modal and static analyses. The results indicate that stress concentrations are primarily located at critical points such as the eccentric connection near the upper frame bearing and the junction between the lower and upper frames, which are particularly susceptible to damage under dynamic loads.

In addition, random vibration analysis was performed in accordance with the IEC 61373-2010 standard under two scenarios: normal operating conditions and simulated fault conditions. The results revealed significant differences in the vibration signals between the intact pantograph and the faulted pantograph under random vibration. These differences, particularly in the frequency shifts and amplitude amplifications at critical stress points, confirm that vibration signal monitoring is an effective method for fault detection in pantographs. By analyzing the vibration characteristics, potential faults can be identified early, providing a theoretical foundation for the development of advanced fault diagnosis techniques.

Looking ahead, this study provides valuable insights into the structural performance and dynamic characteristics of straddle-type monorail pantographs and underscores the importance of vibration-based monitoring as a diagnostic tool. Future research should focus on the following areas:

(1) Experimental validation: conduct real-world experiments to verify the accuracy and reliability of the proposed theoretical and computational methods.
(2) Advanced signal processing: apply advanced techniques such as machine learning and spectral analysis to improve the precision and efficiency of fault detection.
(3) Robust monitoring systems: develop more durable, efficient, and scalable monitoring systems tailored to real-world urban rail transit conditions.

These advancements will contribute to enhancing the reliability, safety, and long-term performance of pantograph systems in urban monorail operations, supporting the increasing demands of modern transportation systems.

Funding information: This work has received partial funding from Young Project of Science and Technology Research Program of Chongqing Education Commission of China (No KJQN202303425) and Chongqing Education Science Planning Project, General Teaching Research Special Project, Research on Teaching Ability of Vocational School Teachers in the Context of Digitalization (No K24ZG3140350).

Author contributions: Conceptualization: S.W. and T.X.; methodology: S.W.; software: S.W. and T.X.; validation: S.W. and T.X.; formal analysis: S.W.; investigation: T.X.; resource: S.W. and T.X.; writing – original draft preparation: S.W.; and writing – review and editing: S.W. and T.X. Both authors have read and agreed to the published version of the manuscript.

Conflict of interest: The authors declared no potential conflicts of interest with respect to the research, authorship, and publication of this article.

Data availability statement: The datasets used and analyzed during the current study are available from the corresponding author on reasonable request.

References

[1] Song J, Zhang L, Zhu D, Liang H. Active control of shimmy in articulated single-axle straddle-type monorail train. Machines. 2024;12(12):854.

[2] Ma Z, Guo Y. Crosswind impacts on comfort of straddle monorail vehicle running on flexible track beam. J Mech Sci Technol. 2024;38(2):569–77.
[3] Wen X, Nie Y, Du Z, Hang L. Operational safety assessment of straddle-type monorail vehicle system based on cloud model and improved CRITIC method. Eng Fail Anal. 2022;139:106463.
[4] Wen X, Huang L, Du Z, Chen L, Yang Z. Research on parameter optimization based on multi-body dynamics model of monorail vehicle aiming at reducing running wheel wear. Proc Inst Mech Eng Part K J Multi-Body Dyn. 2022;236(4):588–601.
[5] Zhou J, Liu Y, Gao J, Liao Y, Du H. Shimmy analysis of straddle-type monorail vehicle with single-axle bogies based on factor model. Veh Syst Dyn. 2024;62(5):1063–84.
[6] Zou J, Chen B, Zhan S, Huang C, Wang X. Theoretical derivation of gauges for straddle-type monorail vehicle. J Phys Conf Ser. 2021;1910(1):012052.
[7] Zhang H, Wang P, Li Q, Jin J, Wei S, Guo F, et al. An experimental and numerical study on the lateral stiffness limits of straddle-type monorail tour-transit systems. Buildings. 2024;14(10):3111.
[8] Guo F, Ji Y, Liao Q, Liu B, Li C, Wei S, et al. The limit of the lateral fundamental frequency and comfort analysis of a straddle-type monorail tour transit system. Appl Sci. 2022;12(20):10434.
[9] Tan Y, Liu R, Wang X, Zhao D, Zen Y. Image segmentation method for monorail pantograph carbon slider based on improved U-Net. Rail Transit Mater. 2024;3(4):63–7.
[10] Li X, Wang J, Su A, Gao W, Wu R, Jia S, et al. Simulation analysis of high-speed train pantographs based on finite element method. Railw Locomot Cars. 2019;39(5):100–3, 130.
[11] Liu C, Di K, Du Z, Yang Z. Research on active control of straddle-type monorail pantograph-contact network coupling. J Chongqing Jiaotong Univ Nat Sci Ed. 2021;40(2):129–35.
[12] Zhou Z, Xiao S, He X, Jian Z, Cai C. Random vibration analysis of straddle-type monorail train-bridge system. J Railw Sci Eng. 2023;20(11):4210–20.
[13] Chen L, Xiong J, Wang S. Study on the sliding mode variable structure semi-active control method for straddle-type monorail pantograph. J Mech Strength. 2023;45(5):1058–64.
[14] Zhou X, Li F, Feng H, Luo J, Li Z. Analysis of the effect of bridge span on the coupled vibration of straddle-type monorail vehicle-bridge system. Noise Vib Control. 2024;44(4):1–7.
[15] Zhang Y, Zhang J. Aerodynamic noise characteristics of pantograph position and the height of the air duct embedded in the vehicle body. J Railw Sci Eng. 2020;42(8):60–7.